JOURNAL OF GEOPHYSICAL RESEARCH, VOL. 115, A04217, doi:10.1029/2009JA014978, 2010

Plasmaspheric EUV images seen from lunar orbit: Initial results of the extreme ultraviolet telescope on board the Kaguya spacecraft

I. Yoshikawa,[1] G. Murakami,[1] G. Ogawa,[1] K. Yoshioka,[1] Y. Obana,[1] M. Taguchi,[2] A. Yamazaki,[3] S. Kameda,[3] M. Nakamura,[3] M. Kikuchi,[4] M. Kagitani,[5] S. Okano,[5] and W. Miyake[6]

Received 13 October 2009; revised 3 January 2010; accepted 17 February 2010; published 27 April 2010.

[1] The Telescope of Extreme Ultraviolet (TEX) aboard Japan's lunar orbiter Kaguya has succeeded in imaging of the plasmaspheric helium ions by detecting resonantly scattered emission at 30.4 nm. After the initial instrumental check was completed, TEX has been operated routinely, and EUV images from TEX have become available from the perspective of the lunar orbit. The view afforded by the Kaguya orbit encompasses the plasma (He^+) distribution in a single exposure, enabling us to examine for the first time the globally averaged properties of the terrestrial plasmasphere from the "side" (meridian) perspective. In this paper we report the inward motion of the nightside plasmapause on 2 May 2008 as seen from this remote meridian view of the Earth. The southward turning of the IMF initiated the inward motion of the plasmapause, and the nightside plasmasphere shrunk at a rate of 0.2 Re/h. Simultaneous solar wind velocity measurements provide a possible explanation for the total radial displacement of the plasmasphere observed in the EUV images.

Citation: Yoshikawa, I., et al. (2010), Plasmaspheric EUV images seen from lunar orbit: Initial results of the extreme ultraviolet telescope on board the Kaguya spacecraft, *J. Geophys. Res.*, *115*, A04217, doi:10.1029/2009JA014978.

1. Introduction

[2] A small extreme ultraviolet (EUV) scanning instrument carried on board the Planet-B (Nozomi) spacecraft performed the first ever imaging of the plasmasphere from outside the terrestrial magnetosphere. This EUV scanner on Nozomi provided static pictures of the plasmasphere [*Nakamura et al.*, 1999, 2000] and demonstrated its evolution during periods of fairly quiet [*Yoshikawa et al.*, 2003] and stormy geomagnetic activity [*Yoshikawa et al.*, 2001c]. This first plasmaspheric EUV imaging has provided a more global perspective of the plasmasphere, and has led us to take more global images of the terrestrial plasma distribution, i.e., plasmasphere, polar wind, and plasma sheet [*Yoshikawa et al.*, 2000b, 2001a]. A few years later, the Imager for Magnetopause-to-Aurora Global Exploration (IMAGE) mission produced consecutive images of the terrestrial plasmasphere from the high-latitude view [*Sandel et al.*, 2000; *Burch et al.*, 2001]. The IMAGE mission identified not only the well-known morphology of the plasmasphere (plasmapause, tails, and duskside bulge), but also described novel structures, e.g., depleted regions that are called "notches" and a radially extended, narrow MLT enhanced-density feature called "finger" [see *Darrouzet et al.*, 2009, and references therein].

[3] Furthermore, the understanding of plasmaspheric dynamics has advanced in many areas, for example determining how rapidly storm time convective electric fields penetrate into the body of plasmasphere. *Goldstein et al.* [2003b] first studied the inward motion of the plasmapause as seen in the EUV images in response to the solar wind electric field which was measured by solar wind monitor (ACE satellite). Later, *Murakami et al.* [2007] found 16 events in the period of May 2000 to December 2001, showing that the inward motion of the plasmapause was driven by the southward turning of IMF. They showed that the plasmapause responds to the southward turning with a delay in the range 10–30 min, and average of 18 min.

[4] While the technological developments required to image terrestrial EUV radiation at 30.4 nm are still in progress [e.g., *Yoshikawa et al.*, 2005], we have built the second-generation extreme ultraviolet telescope for Japan's lunar mission (Kaguya), based on the successful demonstration by two rocket-borne EUV instruments [*Yoshikawa et al.*, 1997; *Yamazaki et al.*, 2002]. The Upper Atmosphere and Plasma Imager (UPI) on Kaguya produces

[1]Department of Earth and Planetary Science, University of Tokyo, Tokyo, Japan.
[2]Department of Physics, Rikkyo University, Tokyo, Japan.
[3]Institute of Space and Astronautical Science, Sagamihara, Japan.
[4]National Institute of Polar Research, Tokyo, Japan.
[5]Planetary Plasma and Atmospheric Research Center, Sendai, Japan.
[6]Department of Aeronautics and Astronautics, Tokai University, Hiratsuka, Japan.

0148-0227/10/2009JA014978

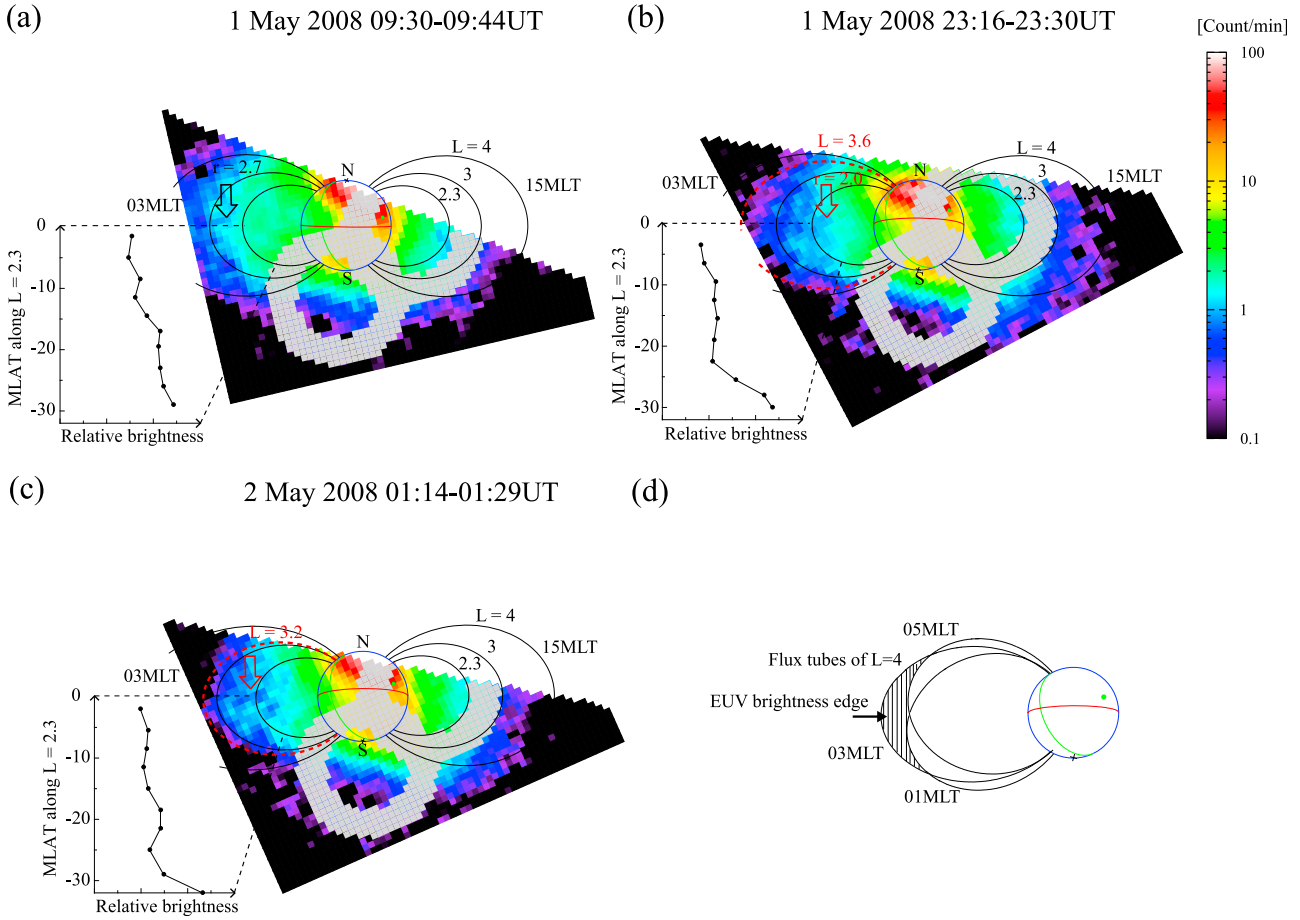

Figure 1. (a–c) Three EUV plasmaspheric images from the meridian view taken on 1–2 May 2008. The inward motion is clearly seen in the nightside. (d) Flux tubes seen from the lunar orbit. The nightside EUV brightness reflects the plasma distribution at 03 MLT rather than adjacent local times.

images of the Earth in the visible and EUV spectral ranges. There are two telescopes, the Telescope for Visible emission (UPI-TVIS) and the Telescope of Extreme Ultraviolet emission (UPI-TEX). UPI-TVIS images the Earth's airglow and aurora at 4 wavelengths [*Taguchi et al.*, 2009] and of the lunar sodium exosphere [*Kagitani et al.*, 2009]. UPI-TEX images the resonantly scattered emissions of oxygen ions at 83.4 nm (O II) and helium ions at 30.4 nm (He II) [*Yoshikawa et al.*, 2008]. Kaguya was launched by the H-IIA rocket in 2007 and inserted into lunar orbit. From lunar orbit, the Kaguya project has carried out both scientific observations of the Moon and from a lunar perspective. In this paper we report the analysis of the initial images of terrestrial He II (30.4 nm) radiation obtained by the UPI-TEX instrument. These first two-dimensional images by Kaguya provide a meridian perspective from outside the magnetosphere. The novel images taken by the other EUV channel (83.4 nm) will be published in a separate paper.

2. Instrumentation and Observation

[5] Images of the plasmasphere have been obtained since 1970s from sounding rockets [e.g., *Meier and Weller*, 1972] and from orbiting spacecraft [*Yoshikawa et al.*, 2000a]. These instruments typically built up an image of the plasmasphere by integrating many separate individual "slit" images (1-D or narrow field-of-view images). Such techniques generally provided images of relatively poor time resolution. High time resolution images of the plasmasphere require global "snapshots" with a wide field of view (FOV). Otherwise, the information in the images may be seriously aliased by motion of the plasmasphere within the imaging period. Kaguya provides an ideal platform commanding a panoramic view of geospace.

[6] The Kaguya satellite has a 2 h orbital period around the Moon. This provides an observation window of the Earth every 2 h. The following geometrical conditions determine a period of the observation window per orbit:

[7] 1. The satellite has a clear view of the Earth.

[8] 2. The satellite is in the umbra of the Moon, thus reducing stray sunlight incident on TEX.

[9] The periods of observation windows in May 2008 (Figure 1) were each of approximately 14–15 min duration. While the EUV images in Figure 1 were obtained, the Moon was in the Earth's magnetic equatorial plane (from +1° to −10° MLAT). The viewing direction of TEX on the Earth was perpendicular to the meridian plane of 3–15 MLT. *Yoshikawa et al.* [2008] showed that an exposure of approximately 10 min duration was necessary to obtain one image with the maximum high voltage level applied to the

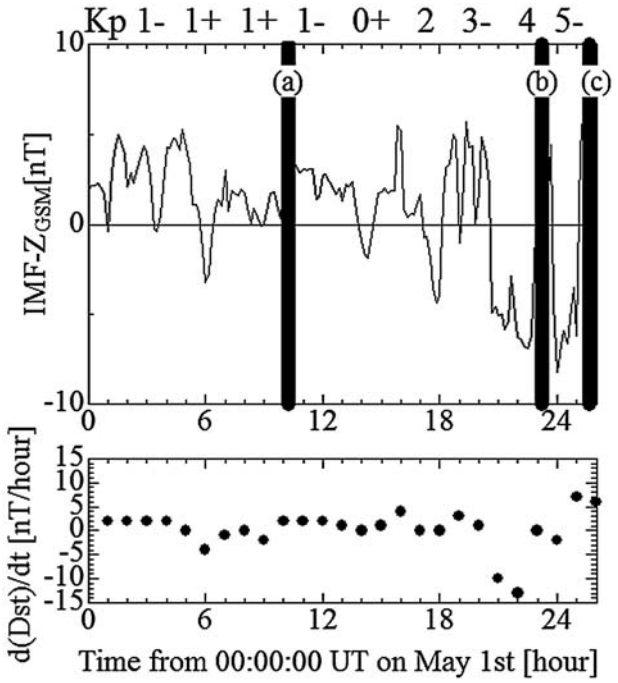

Figure 2. IMF z component obtained by the ACE measurement, Kp index, and the time derivative coefficient of Dst. The ACE data are presented with a 1 h time delay to compensate for the propagation from the measurement point to the Earth. The observation windows for Figures 1a, 1b, and 1c are indicated by vertical bars.

detector. However, in this paper we integrate all the images taken during one orbit to increase signal-to-noise ratio.

[10] The TEX instrument is mounted on a two-rotational-axis gimbal system together with TVIS. The rotation around the azimuthal (AZ) axis cancels the apparent drift motion of the Earth in the image due to the orbital motion of the spacecraft about the Moon. The other rotation (EL: elevation axis) cancels changes in the apparent declination of the Moon. As the result of both rotations, the Earth can always be kept in the center of FOV, providing images of the Earth's plasmasphere every minute. The TEX instrument is a type of normal-incidence telescope with a spatial resolution of 0.1 Re, using Mo/Si multilayer coated mirror and a split thin metal filter. These optical components are technologically identical to those used in previous space-borne instruments [*Yoshikawa et al.*, 1997, 2001b]. The filter is made of Aluminum/Carbon and Indium and transmits the resonance scattering emissions of helium ions (He II) and oxygen ions (O II). The key point for He II (30.4 nm) imaging is to eliminate geocoronal emissions at maximum intensities of 10 kR (H I 121.6 nm) [*Rairden et al.*, 1986] and of 100 R (He I 58.4 nm) [*Meier and Weller*, 1972]. The preflight calibration showed that both emissions are sufficiently reduced or eliminated by the filter for the plasmaspheric imaging [*Yoshikawa et al.*, 2008].

[11] After the primary function checks of the complete spacecraft and instrument, the high voltage power supply was turned on 1 May 2008. The metal band-pass filter was found to be mechanically damaged. This might have been due to vibration or shock during the vehicle launch phase. Two small pinholes on the filter were identified. The exact locations of these pinholes were investigated during the EUV star calibration. A circular "ghost" appeared on all EUV images due to the leak of geocoronal emissions from longer wavelength. The "ghost" location is stable in all EUV images and is therefore predictable by calculation, independent of plasmaspheric morphology. This simplifies the image correction and image analysis and ensures our study without additional care. In this paper, all pixels which were potentially contaminated by the artificial signals have been removed.

3. Inward Motion of the Outer Boundary in the Nightside During a Disturbed Period

[12] There was a succession of geomagnetically quiet days in 2008. Fortunately, UPI-TEX has produced meridian plasmasphere images during a geomagnetically disturbed period from 1 to 2 May.

[13] Figures 1a–1c show three EUV snapshots. The apparent size and location of the Earth, the equator (red lines), the day-night terminator (green lines), and subsolar point (green dots) are indicated. Due to the operational limitations, no images were available between the interval between Figures 1a and 1b. The dipole magnetic field lines at 03 and 15 MLT are shown. The sharp He^+ edges in the nightside are identified in Figures 1b and 1c. The nightside edges are aligned to L shells of L = 3.6 and L = 3.2 at 03 MLT, respectively (red broken lines). As for the EUV outer boundary, *Goldstein et al.* [2003a] performed a specific study in comparing the location of the outer boundary observed by IMAGE-EUV with in situ data, in order to verify that the observed edge is indeed the plasmapause. Their result is valid only for the IMAGE-EUV instrument as they depend highly on the lower sensitivity threshold of the instrument. Although a study analogous to that of *Goldstein et al.* [2003a] needs to be performed for UPI-TEX, we assume that the sharp He^+ edge does correspond to the plasmapause.

[14] Because the brightness edge consists of the outermost L shell in the plasmasphere, (the nightside EUV radiation at the edge in Figure 1d comes from the plasmasphere at 03 MLT rather than adjacent local times), if we assume a featureless and azimuthally smooth plasmapause at the nightside, the edges should be interpreted as the plasmapause with L = 3.6 at 03 MLT in Figure 1b and with L = 3.2 at 03 MLT in Figure 1c.

[15] *Carpenter and Anderson* [1992] modeled the plasmapause location using the maximum of Kp over an interval of several hours and up to a day prior to the observation. The predicted location (L_{pred}) is 3.7 for the Figure 1b period and 3.3 for the Figure 1c period. On the other hand, *O'Brien and Moldwin* [2003] developed models of the plasmapause location using other geomagnetic indexes (AE and Dst). We calculated L_{pred} based on series of Dst as 4.3 for the Figure 1b period and 4.2 for the Figure 1c period, and on AE index L_{pred} = 4.2 for the Figure 1b and 1c periods. The predictions by Dst- and AE-dependent models correspond less precisely to the plasmapause position as seen from the meridian view than the Kp-dependent model.

[16] Figure 2 displays the summary of the IMF-z, the Kp index, and the time derivative coefficient of Dst (nT/h). A

10 min average of the IMF data is used because the plasmaspheric response to IMF takes 10–30 min [*Murakami et al.*, 2007], and the data are time delayed by 56 min to account for propagation to the Earth's magnetopause, assuming the solar wind speed is 450 km s^{-1}. The IMF is clearly northward until 18 UT on 1 May. The geomagnetic activity was quite low with average Kp of 1. A gradual decrease of brightness (density) with increasing L shell is seen in Figure 1a, as is typically seen in our EUV images of the plasmasphere obtained after prolonged periods of low geomagnetic activity. The earlier successful mission IMAGE-EUV produced EUV images over several years, and *Goldstein et al.* [2005] reported a similar behavior as seen from a high-latitude perspective by IMAGE-EUV during periods of low to moderate activity.

[17] From 20 UT to 23 UT on 1 May, the IMF polarity turned to southward, and the geomagnetic activity (Kp) increased up to 5-. Dst decreased with a rate of 10 [nT/h] at 21 UT. Comparing the three EUV images in Figure 1, it is clear that the nightside plasmapause moved inward from L = 3.6 toward L = 3.2. It is likely that the enhanced convection electric field triggered by the southward turning of the IMF generated a new E × B drift trajectory. The diffuse EUV outer boundary at the nightside (Figure 1a) then began moving inward, forming a clear boundary. If we compare the outermost L shells described in Figures 1b and 1c, the mean speed was approximately 0.2 Re/h and the total displacement was about 0.4 Re on the equatorial plane. The determination of the plasmapause location is some ambiguous, since the manual plotting of the outer EUV boundary is somewhat subjective. Five of the authors of the paper performed plasmapause extractions from selected images for practice. We found the subjectivity to be ± 0.1 Re. The subjective error is smaller than the total displacement, and we estimate the mean inward speed with uncertainty as 0.2 ± 0.1 Re/h. The mean speed of the EUV outer boundary, deduced from the data obtained during a similar geomagnetic trend on 10 July 2000, was 0.6 Re/h [*Goldstein et al.*, 2005]. This is not inconsistent with our result.

[18] Simultaneous ACE measurement showed that z component of IMF (Bz) was −6 nT and that solar wind velocity (Vx) was 450 km/s on average during the period the images in Figures 1b and 1c were taken. Therefore, the induced electric filed (Esw) across the magnetosphere was Esw = −Vx × Bz = 2.7 mV/m. If twenty percent (assumed) of this electric field was induced across the magnetosphere [*Murakami et al.*, 2007], the inward plasmapause velocity (Vpp) at L = 3.5 was estimated by Vpp = 0.2 × Esw × B_{dip} = 0.74 km/s = 0.42 Re/h, where B_{dip} is the dipole magnetic strength at L = 3.5 on the equator. The southward polarity of the IMF continued for 80 min (from 23:40–25:00) and the plasmapause was expected to move inward by 0.56 Re. This estimation has agreement with the value deduced from the observations.

[19] In the nightside on the equatorial plane, the plasmaspheric EUV radiation in Figure 1a is relatively low in comparison with that in higher latitudes. This low brightness is due to the Earth's shadow effect. On the other hand, the density depletion is more significant in Figures 1b and 1c (see red arrows). The brightness is plotted along L = 2.3 (the innermost field line in the image) at 03 MLT for each image. The equatorial brightness becomes lower than that at higher latitudes in Figures 1b and 1c, while a less significant depletion is seen in Figure 1a. The plasmaspheric density profile on the meridian plane varies from Figure 1a to Figure 1b.

[20] An apparently related phenomenon was reported by *Oya* [1997]. Oya studied electron density profiles obtained by the polar orbiter (EXOS-D) with an apogee of 10,000 km. On some orbits during periods of recovery after disturbances, regions of depressed plasma densities were found near the equator at L = 2.5. When apogee was near the equator, the corresponding electron density profiles versus time exhibited conjugate density peaks at off-equatorial latitudes, indicating a belt of higher-density plasma beyond L = 2.5. The off-equatorial peaks were described as "donkey ears" and *Oya* [1997] proposed the betatron drift theory to explain their nature [*Oya*, 1997]. He interpreted the plasmasphere behavior as a function of magnetic field variation in term of the plasma drift caused by the time varying electric field generated by the time-dependent variation of the ring current. According to his study, the plasmaspheric plasma is eroded toward the plasma sheet region during a phase of decreasing Dst. It is characterized by the intimate correspondence to the time variation of Dst that indicates the time derivative coefficient smaller than −5 [nT/h]. It should be noted in our observation that Dst decreased at the rate of more than 10 [nT/h] 3 h before Figure 1b was taken as shown in Figure 2 (bottom). Based on the *Oya* [1991] study, we calculate the period (T) of the plasma erosion starting from r = 2.7 in Figure 1a to r = 2.0 in Figure 1b with $dDst/dt$ = −10 [nT/h], then we have T = 3.2 [h]. A possible scenario is that the plasmaspheric plasma near the equator started to be peeled off toward the plasma sheet at 20 UT, by 23 UT plasma at r = 2.0 was eroded, when Figure 1b was obtained. This scenario is not exclusive, but this is the first meridian image of such a plasmaspheric density depletion.

4. Conclusion

[21] EUV images from the new perspective of lunar orbit have become available. Our Kaguya-EUV images will mostly be used to study of plasmaspheric dynamics in combination with data from IMAGE-EUV. We have reported the inward motion of the plasmapause in the night side during the disturbed period on 1–2 May 2008. From the meridian view, we have determined that the inward speed is 0.2 Re/h on the assumption that the plasmapause was featureless and azimuthally smooth on the nightside. This result is consistent with the estimate based on simultaneous measurements of the solar wind velocity.

[22] We have also identified the plasma depletion in the plasmasphere during a phase of decreasing Dst. This might be the "donkey ears" phenomenon which is often identified by in situ electron density measurements within the plasmasphere. Because the instrument was not operated routinely in May 2008, the observation coverage was imperfect. We believe that the betatron drift theory is able to explain the nature of the plasma depletion observed in the equatorial plane.

[23] While these features, i.e., the inward motion of the plasmapause and plasma depletion near the equatorial plane, have been reported previously, the TEX instrument is novel in that it images the plasmasphere from a remote meridian

perspective. It thus has the potential to extend the capabilities of previous observations. The side-view images provide a major advantage in terms of visualizing the plasma depletion scenario. *Obana et al.* [2010] has used this advantage to study the refilling of the plasmasphere.

[24] The instrumental check has now been completed, TEX is being operated, and images from Kaguya-EUV have been routinely produced and are available to monitor the behavior of the plasmasphere.

[25] **Acknowledgments.** Masaki Fujimoto thanks the reviewers for their assistance in evaluating this paper.

References

Burch, J. L., et al. (2001), Views of Earth's magnetosphere with the IMAGE satellite, *Science*, *291*, 619–624.

Burch, J. L., J. Goldstein, and B. R. Sandel (2004), Cause of plasmasphere corotation lag, *Geophys. Res. Lett.*, *31*, L05802, doi:10.1029/2003GL019164.

Carpenter, D. L., and R. R. Anderson (1992), An ISEE/Whistler model of equatorial electron density in the magnetosphere, *J. Geophys. Res.*, *97*, 1097–1108.

Darrouzet, F., J. De Keyser, and V. Pierrard (Eds.) (2009), *The Earth's Plasmasphere: A Cluster and Image Perspective*, Springer, Heidelberg, Germany.

Goldstein, J., M. Spasojević, P. H. Reiff, B. R. Sandel, W. T. Forrester, D. L. Gallagher, and B. W. Reinisch (2003a), Identifying the plasmapause in IMAGE EUV data using IMAGE RPI in situ steep density gradients, *J. Geophys. Res.*, *108*(A4), 1147, doi:10.1029/2002JA009475.

Goldstein, J., B. R. Sandel, W. T. Forrester, and P. H. Reiff (2003b), IMF-driven plasmasphere erosion of 10 July 2000, *Geophys. Res. Lett.*, *30*(3), 1146, doi:10.1029/2002GL016478.

Goldstein, J., B. R. Sandel, W. T. Forrester, M. F. Thomsen, and M. R. Hairston (2005), Global plasmasphere evolution 22–23 April 2001, *J. Geophys. Res.*, *110*, A12218, doi:10.1029/2005JA011282.

Kagitani, M., M. Taguchi, A. Yamazaki, I. Yoshikawa, G. Murakami, K. Yoshioka, S. Kameda, F. Ezawa, T. Toyota, and S. Okano (2009), First optical observation of the Moon's sodium exosphere from the lunar orbiter SELENE (Kaguya), *Earth Planets Space*, *61*, 1025–1029.

Meier, R. R., and C. S. Weller (1972), EUV resonance radiation from helium atoms and ions in the geocorona, *J. Geophys. Res.*, *77*, 1190–1204.

Murakami, G., M. Hirai, and I. Yoshikawa (2007), The plasmapause response to the southward turning of the IMF derived from sequential EUV images, *J. Geophys. Res.*, *112*, A06217, doi:10.1029/2006JA012174.

Nakamura, M., K. Yamashita, I. Yoshikawa, K. Shiomi, A. Yamazaki, and S. Sasaki (1999), Helium observation in the Martian ionosphere by an X-ray ultraviolet scanner on Mars orbiter NOZOMI, *Earth Planets Space*, *51*, 61–70.

Nakamura, M., I. Yoshikawa, A. Yamazaki, K. Shiomi, Y. Takizawa, M. Hirahara, K. Yamashita, Y. Saito, and W. Miyake (2000), Terrestrial plasmaspheric imaging by an extreme ultraviolet scanner on Planet-B, *Geophys. Res. Lett.*, *27*(2), 141–144.

Obana, Y., G. Murakami, I. Yoshikawa, I. R. Mann, P. J. Chi, and M. B. Moldwin (2010), Conjunction study of plasmapause location using ground-based magnetometers, IMAGE-EUV, and Kaguya-TEX data, *J. Geophys. Res.*, doi:10.1029/2009JA014704, in press.

O'Brien, T. P., and M. B. Moldwin (2003), Empirical plasmapause models from magnetic indices, *Geophys. Res. Lett.*, *30*(4), 1152, doi:10.1029/2002GL016007.

Oya, H. (1997), Dynamical variation of plasmasphere revealed by PWS data onboard the Akebono (EXOS-D) satellite, *J. Geomagn. Geoelectr*, *49*, S159–S178.

Rairden, R. L., L. A. Frank, and J. D. Craven (1986), Geocoronal imaging with Dynamics Explorer, *J. Geophys. Res.*, *91*, 13,613–13,630.

Sandel, B. R., et al. (2000), The Extreme Ultraviolet Imager Investigation for the IMAGE mission, *Space Sci. Rev.*, *91*(1/2), 197–242.

Taguchi, M., et al. (2009), The Upper Atmosphere and Plasma Imager/the Telescope of Visible Light (UPI/TVIS) onboard the Kaguya spacecraft, *Earth Planets Space*, *61*, xvii–xxiii.

Yamazaki, A., S. Tashiro, Y. Nakasaka, I. Yoshikawa, W. Miyake, and M. Nakamura (2002), Sounding-rocket observation of O II 83.4-nm emission over the polar ionosphere, *Geophys. Res. Lett.*, *29*(21), 2005, doi:10.1029/2002GL014788.

Yoshikawa, I., M. Nakamura, M. Hirahara, Y. Takizawa, K. Yamashita, H. Kunieda, T. Yamazaki, K. Misaki, and A. Yamaguchi (1997), Observation of He II emission from the plasmasphere by a newly developed EUV telescope on board sounding rocket S-520-19, *J. Geophys. Res.*, *102*, 19,897–19,902.

Yoshikawa, I., A. Yamazaki, K. Shiomi, K. Yamashita, Y. Takizawa, and M. Nakamura (2000a), Evolution of the outer plasmasphere during low geomagnetic activity observed by the EUV scanner onboard Planet-B, *J. Geophys. Res.*, *105*, 27,777–27,789.

Yoshikawa, I., A. Yamazaki, K. Shiomi, K. Yamashita, Y. Takizawa, and M. Nakamura (2000b), Photometric measurement of cold helium ions in the magnetotail by an EUV scanner onboard Planet-B: Evidence of the existence of cold plasmas in the near-Earth plasma sheet, *Geophys. Res. Lett.*, *27*(21), 3567–3570.

Yoshikawa, I., A. Yamazaki, K. Shiomi, M. Nakamura, K. Yamashita, Y. Saito, M. Hirahara, Y. Takizawa, W. Miyake, and S. Matsuura (2001a), Development of a compact EUV photometer for imaging the planetary magnetosphere, *J. Geophys. Res.*, *106*(A11), 26,057–26,074.

Yoshikawa, I., A. Yamazaki, K. Shiomi, K. Yamashita, Y. Takizawa, and M. Nakamura (2001b), Interpretation of the He II (304Å) EUV image of the inner magnetosphere by using empirical models, *J. Geophys. Res.*, *106*, 25,745–25,758.

Yoshikawa, I., A. Yamazaki, K. Shiomi, K. Yamashita, Y. Takizawa, and M. Nakamura (2001c), Loss of plasmaspheric ions during a storm observed by the EUV scanner onboard Planet-B, *J. Geophys. Res.*, *106*, 18,911–18,918.

Yoshikawa, I., A. Yamazaki, K. Yamashita, Y. Takizawa, and M. Nakamura (2003), Which is a significant contributor for outside of the plasmapause, an ionospheric filling or a leakage of plasmaspheric materials?: Comparison of He II (304Å) images, *J. Geophys. Res.*, *108*(A2), 1080, doi:10.1029/2002JA009578.

Yoshikawa, I., T. Murachi, H. Takenaka, and S. Ichimaru (2005), Multilayer coating for 30.4 nm, *Rev. Sci. Instrum.*, *76*(6), 066109, doi:10.1063/1.1938867.

Yoshikawa, I., et al. (2008), Telescope of extreme ultraviolet (TEX) onboard SELENE: Science from the Moon, *Earth Planets Space*, *60*, 407–416.

M. Kagitani and S. Okano, Planetary Plasma and Atmospheric Research Center, 6-3 Aramaki-aza-aoba, Aoba, Sendai, 980-8578, Japan. (kagi@pparc.geophys.tohoku.ac.jp; okano@pparc.geophys.tohoku.ac.jp)

S. Kameda, M. Nakamura, and A. Yamazaki, Institute of Space and Astronautical Science, 3-1-1 Yoshinodai, Sagamihara, Kanagawa, 229-8510, Japan. (kameda@stp.isas.jaxa.jp; nakamura@stp.isas.jaxa.jp; yamazaki@stp.isas.jaxa.jp)

M. Kikuchi, National Institute of Polar Research, 9-10-1 Kaga, Itabashi, Tokyo, 173-8515, Japan. (kikuchi@nipr.ac.jp)

W. Miyake, Department of Aeronautics and Astronautics, Tokai University, 1117 Kitakinme, Hiratsuka, Kanagawa, 259-1292, Japan. (wmiyake@keyaki.cc.u-tokai.ac.jp)

G. Murakami, Y. Obana, G. Ogawa, I. Yoshikawa, and K. Yoshioka, Department of Earth and Planetary Science, University of Tokyo, 7-3-1 Hongo, Bunkyo, Tokyo, 113-0033, Japan. (go@eps.s.u-tokyo.as.jp; obana@eps.s.u-tokyo.as.jp; ogawa@eps.s.u-tokyo.as.jp; yoshikawa@eps.s.u-tokyo.as.jp; yoshioka@eps.s.u-tokyo.as.jp)

M. Taguchi, Department of Physics, Rikkyo University, 3-34 Nishiikebukuro, Toshima, Tokyo, 171-8501, Japan. (taguchi@rikkyo.as.jp)